

## **Axonal endoplasmic reticulum is very narrow**

Mark Terasaki  
Department of Cell Biology  
University of Connecticut Health Center  
Farmington, CT 06030  
terasaki@uchc.edu

### **Summary Statement**

Using new methods of serial section electron microscopy, the axonal ER is found to consist of unusually narrow tubules compared to ER tubules found in other cells.

### **Abstract**

The endoplasmic reticulum (ER) is an interconnected network of tubules and sheets. In most tissues of the body, ER tubules have a diameter of ~60 nm. Using new methods for serial section electron microscopy, a distinct class of very narrow, 20-30 nm diameter tubules were found in neurons of both the central and peripheral nervous system. The narrow tubules appear to be the most abundant form of ER in axons, and are also found interspersed in the cell bodies and dendrites. At the site of branch points, there is a small sheet which has a similarly narrow lumen. The narrowness of the ER is likely to be important for the as yet poorly characterised functions of the axonal ER.

## Introduction

The endoplasmic reticulum (ER) was first seen as a two dimensional network in the thin periphery of cells growing on formvar coated electron microscopy grids (Porter et al., 1945). Several years later, this network (“reticulum”) was given its name because it was abundant in the non-spreading regions (“endoplasm”) and scarce or absent in the spreading regions of the fibroblasts (ectoplasm) (Porter, 1953). The development of the ultramicrotome enabled inspection of cells in tissues, where the ER was found to be a complex three dimensional system of interconnecting tubules and cisternae (sheets) (Porter and Blum, 1953).

A very active period of investigation established the appearance of the ER in many cell types and organisms (Fawcett, 1981). However, this pertains to the ER only as it appears in single sections, because it is difficult to collect and image serial sections by the classical methods of thin section electron microscopy. As a result, there are still many questions regarding the three dimensional and higher order organization of the ER.

There are two relatively recent developments which enable progress on understanding ER structure. One is the discovery of curvature inducing proteins in the ER (Voeltz et al., 2006). This has been able to explain differences between tubules and sheets, and generally shows that cells can control the shape of the ER for different purposes. Inter-relationships of the different curvature proteins and how they give rise to ER shape are currently being investigated (e.g., Powers et al., 2017). The second development is of new methods for serial section electron microscopy (Denk and Horstmann, 2004; Kasthuri et al., 2015; Wu et al., 2017). These methods were developed in order to determine the synaptic connectivity in neuronal tissue but are also useful for the ultrastructure of cells and tissues in general. Using the ATUM method (Kasthuri et al., 2015), helicoidal ramps that connect ER sheets were discovered in parotid salivary glands (Terasaki et al., 2013). With this method, a characteristic type of ER tubules was found in neuronal cells.

## Results

### Narrow ER tubules in neurons

The ATUM method was used to generate 100-200 serial sections 40-60 nm thick of several mouse organs, including salivary parotid gland, ovarian follicles, duodenum, adrenal cortex, spinal cord, and brain. The original ATUM data set was also examined; it consists of 1850 sections, 30 nm thick from mouse cortex, layer 4/5 (Kasthuri et al., 2015).

The serial section data allows unambiguous identification of tubular ER which often cannot be distinguished from vesicles in single sections. In non-neuronal cells, the tubular ER is frequently present and has a diameter of ~60 nm. For example, the intercalated ducts of the salivary gland contain a network of smooth ER in the cytoplasm next to the lumen. The tubules narrow or widen for a few sections at most (each section is 30 nm thick), the smallest diameters are ~25 nm, and the largest are ~90 nm (Figure 1). From examples of tubular ER in ultrastructural atlases (e.g. Fawcett, 1981), these diameters are typical of tubular ER in cells in most tissues.

The ER was examined in several neuronal cell bodies (pyramidal neurons of the cortex, bushy neurons of the anterior ventral cochlear nucleus, and spinal motor neurons). The ER resembles that of non-neuronal cells except for the presence of a relatively small population of very narrow tubules. The narrow tubules appear as a black spot; the staining protocol enhances membrane contrast, and the lower resolution of the scanning electron microscope results in an obscured lumen. In the cell bodies and dendrites, they are unbranched with a diameter that varies between about 15 and 30 nm, and are continuous with the rest of the ER (Figure 2).

Narrow tubules form a small fraction of the ER in the cell body (Figure 3A) but are the most abundant form of ER in axons. The myelinated axons of the white matter of the spinal cord all contain narrow ER (Figure 3B). In cortex, the smallest axons, which are unmyelinated and have a diameter of about 200 nm, usually contain a single narrow tubule (Figure 4). ER in axons of autonomic neurons of the parotid salivary gland are also narrow (Figure 5).

In serial section, the narrow ER tubules usually remain narrow for many sections but sometimes widen to a diameter of 40-60 nm. Tubule branching is relatively frequent. At branch sites, the narrow tubules do not connect to each other directly but instead connect to a small sheet (also called cistern) (Figure 6). The lumen of the sheets have are similarly narrow as the narrow tubules. The tubules connect to the sheet at the edge, rather than perpendicularly to the flat part of the sheet. Free ended tubules are also present (Figure 6).

When axons are viewed in serial section, the density of ER is relatively constant. It seems that the branching and free ends should balance, otherwise the ER density would increase or decrease. In order to investigate this, the numbers of tubules, branches and free ends were counted in consecutive sections over 10 microns distance. Single, myelinated thalamocortical axons of about 0.7  $\mu\text{m}$  diameter pass through mouse layer 4/5 cortex at various angles; the anterograde/retrograde orientation cannot be determined from the data. 30 axons that passed through in cross section were selected; this orientation is easier to analyze than longitudinal sections. For each axon, 360 sections, corresponding to 10.8 microns length, were analyzed.

The number of ER profiles was counted in each section (Fig. 7). The average number of profiles was  $2.99 \pm 0.91$  (std dev) per section (N=10,800 sections). The fluctuation in profile number is caused by the joining / splitting at branches and the appearance / disappearance of free ends. The branches and free ends were identified and counted (Table 1). There were roughly 2 branches per  $\mu\text{m}$  axon in which the number of ER profiles increased in the direction of increasing section number (splitting) balanced by roughly 2 branches per  $\mu\text{m}$  axon in which the number of ER profiles decreased in the direction of increasing section number (combining). Similarly there were roughly 0.5 free ends that appeared per  $\mu\text{m}$  axon and 0.5 free ends that disappeared. The increases and decreases were approximately the same for both branches and free ends; this is consistent with maintaining a constant average number of ER profiles along the length of the axon.

In almost the entire data set, the narrow tubules are interconnected with each other in one continuous structure from the beginning of the serial section series to the end. However, in one axon, there was a 5 section stretch (150 nm) where there were no ER profiles (Figure 7, upper right corner; see also Supplemental Figure 7). In this axon, therefore, the ER is not continuous along the observed length.

## Discussion

Although cellular ultrastructure has been intensively investigated by transmission electron microscopy for more than 50 years, there are many uncertainties regarding three dimensional organization of intracellular membranes. This is due to the difficulty of obtaining and imaging more than one thin section at a time by the classical methods. New automated methods now make serial section electron microscopy much more straight forward. These methods were developed for documenting synaptic connectivity in the central nervous system, but at a smaller scale, the methods should be useful as well for issues of intracellular organization.

Tubular membranes can now be distinguished from vesicles using serial section EM. Tubular ER of diameter 20-30 nm compared to the 50-60 nm found in non-neuronal cells to be present in neurons, especially in axons. In retrospect, narrow tubules were imaged in classic thin section transmission electron micrographs of mammalian axons (Peters et al., 1991), but in single sections, they are impossible to distinguish from small vesicles and were not identified as parts of the ER.

Narrow tubules have been observed in reconstitution studies with ER curvature inducing proteins. Purified recombinant reticulon YOP1/2 protein added to proteolipid planar membranes causes them to become very narrow, 17 nm diameter tubules (Hu et al., 2008). The authors commented that narrow tubules are not seen in cells and that they might be due to unnaturally high levels of curvature inducing proteins that have become incorporated into the membranes (Hu et al., 2008). Now that narrow tubules have been observed in neurons, it seems likely that these ER membranes have incorporated curvature inducing proteins to a similar degree as seen in the reconstitution studies.

### Axonal ER structure

Thick, 1 micron sections of bullfrog spinal motor neurons were examined by high voltage EM (Lindsey and Ellisman, 1985). This showed a branching tubular network that was continuous with the ER in the cell body. The new serial section views of mouse axons document a similar ER network.

The axonal ER is primarily tubular. Tubular membranes don't necessarily have to branch. For example, the axonal plasma membrane geometrically is a long unbranched tube for most of its length. The pattern of ER branching affects the density of the axonal ER. If an ER tubule branches to two tubules, the density of axonal ER increases. The presence of free ends in the axonal ER likewise affects the density of the axonal ER. When viewed in serial section, the axonal ER density appears to be relatively constant along the length of the axon.

To investigate the relative effects of branching and free ends on axonal ER density, the number of branches and free ends were counted along 10 micron segments of axon. Branches occurred at ~2 per micron, and those that increased the density were balanced by an approximately equal number that decreased the density. Free ends were present less frequently than branches, at ~0.5 per micron. They also balanced out. Whatever determines the formation of branches and free ends seems to balance so that the density remains relatively constant in the axon.

The branch points of axonal ER occur where narrow tubules connect to the edges of small sheets (Figure 6). In conventional networks of ER tubules, the tubules form three way junctions (e.g. Terasaki et al., 1986). The narrow tubules do not make this type of junction, possibly because of curvature constraints. Because axonal ER tubules connect at sheet edges, possibly the formation of sheets is a key event, because it provides a location where new tubules can form and other tubules can fuse. The small sheets at the tubule intersections have a narrow lumen. Cisternae with narrow lumens are also seen adjacent to the plasma membrane in some neuronal cell bodies (Wu et al., 2017).

ER movements cannot be studied by serial section EM. This has been studied in the thin periphery of cultured fibroblasts, where the ER can be directly imaged in living cells. In some regions, the ER is rather static but in other regions can undergo rapid and extensive rearrangements, extensions and retractions (e.g. Grigoriev et al., 2008; Nixon-Abell et al., 2016). The ER in axons seems very likely to be dynamic but it is not known to what degree.

Continuity is a very important property of ER membranes. It would be very interesting to know whether the ER is continuous from the cell body throughout the entire axon. Serial section electron microscopy is an excellent method for determining local continuity because the ER membranes are viewed directly. In 30 axons measured over 10.8  $\mu\text{m}$  lengths, the ER was continuous except for a 150 nm interval (Figure 7). Serial section electron microscopy is less well suited for global continuity because of the effort required to generate large volume data sets. Photobleach recovery of fluorescent proteins in the ER membrane or lumen or spreading of lipophilic dyes such as Dil generally does not resolve ER membranes but is nevertheless effective at evaluating continuity. Due to limitations in resolution of light microscopy, these methods are better suited for continuity over larger distances, and have even been used at the level of whole cells (e.g. Terasaki et al., 1996; Ellenberg et al., 1997) though not of whole neurons. In chick dorsal root ganglion axons in culture, photobleaching recovery of GFP chimeras expressed in the ER was consistent with continuity in a 70  $\mu\text{m}$  field of view (Aihara et al., 2001). A recent study demonstrated continuity of ER membranes in *Drosophila* axons over a

similar field of view (Yalçin et al., 2017). The issue of continuity along the entire axon remains to be addressed.

Another topic of interest is the transition of ER organization between the cell body and the axon, which occurs at the axon hillock region. It is not known whether the axonal ER moves as a whole down the axon, and this would be affected by whether the ER moves into the axon at the axon hillock. The presence of narrow tubular ER in the cell body suggests that these are somehow selected to enter the axon.

#### Axonal ER function

The function of axonal ER should be considered in context of the unusual cell biological features of the axon. The axon can be very long, is capable of transporting membranes and proteins along its entire length, can find targets during growth, supports synaptic transmission, and can regrow if injured. The ER could very well have important roles in any or all of these axonal processes. Several well established functions of the ER in fact have been detected in axons, such as lipid synthesis (Gould et al, 1983; Posse de Chaves et al., 1995), calcium regulation (de Juan-Sanz et al., 2017) and protein synthesis (Verma et al., 2005; Shigeoka et al., 2016). However, how the ER participates in axonal growth and homeostasis is far from understood due to the experimental challenges of studying relatively slow processes. Furthermore, neurons have particularly complex structural and functional inter-relationships with other neurons and with glia, so that it is difficult to study normally functioning axons in situ or to approximate this in cell culture systems. Biochemical studies on axons are very difficult, and even with the tremendous technical advances in light microscopy, it is difficult to resolve the axonal ER or monitor its functions.

Axonal ER recently became of interest due to the identification of mutations which cause the human disease Hereditary Spastic Paraplegia (Blackstone, 2012). Patients undergo adult onset degeneration of the longest axons in the body, typically those of the upper spinal motor neurons. The most frequently occurring mutations affect curvature inducing proteins of the ER so that the axonal ER structure seems very likely to be altered. Recent studies in *Drosophila* have found evidence for this. Mutations of ER curvature inducing proteins cause behavioral defects in adult flies consistent with axon degeneration (O'Sullivan et al., 2012). In axons of third instar larvae, the diameter of axonal ER is increased and there are more discontinuities in ER (Yalçin et al., 2017).

How might changes in ER diameter and continuity be related to axon degeneration? Like the mouse axonal ER, the axonal ER tubules in *Drosophila* larvae are also comparatively narrow (~40 nm), and the diameter widens in knockouts of spastic paraplegia proteins (Yalçin et

al., 2017). It might be useful to focus on the unusual narrowness of axonal ER to understand the disease as well as the function of the ER in healthy axons. Possibly, the narrowness is important for controlling the network structure; changes in the branching or free end formation could affect the density of the ER and subsequently affect long term maintenance of the axon. There are certainly other possibilities. The narrowness could help to control the localization of membrane proteins within the ER. The high curvature could restrict or attract different proteins. In cultured mammalian cells, the normally occurring luminal ER proteins such as calreticulin were “squeezed out” when curvature inducing proteins were over-expressed (Hu et al., 2008). The narrowness of the tubule could be significant for establishing ion gradients or allowing electrophoresis of proteins along the ER tubule (Jaffe, 1977). A narrower tubule has a higher electrical resistance in its lumen and therefore a larger length constant. As a result, a localized flux of ions through channels in the ER membrane could establish a larger voltage drop between two regions of the tubule. There is increasing appreciation of organelle interactions such as between ER and mitochondria and how they could be disrupted in disease (e.g. Villegas et al., 2014).

In summary, the new automated methods for serial section microscopy provides data on three dimensional organization of cells that is essential for understanding their function. A very narrow tubule of ER is found to be present in neurons and may play an important role in the axon where it is particularly abundant. Because the narrowness is likely due to several of the proteins implicated in Hereditary Spastic Paraplegia, a more thorough analysis of axonal ER tubules and their interactions with other membranes as well as analysis of spastic paraplegia gene modifications on axonal ER in other model organisms could help to explain the degeneration of long axons that occurs in this disease.

## Materials and Methods

The mouse cortex data was part of the dataset generated in the initial study using the ATUM technique (Kasthuri et al., 2015). The dataset consists of 1850 sections at 30 nm thickness (50  $\mu$ m total depth), with a 50  $\mu$ m x 50  $\mu$ m field of view imaged at 3 nm per pixel (16,000 x 16,000 pixels). The entire data set is available online at <http://www.openconnectomeproject.org>. The data in figures 2, 4, 6 and 7 were selected using the large field of view program Piet (Duncan Mak, Harvard).

For figures 1, 3, 5 and 8, mouse tissues were fixed by cardiac perfusion of fixative, which consisted of 2.5% glutaraldehyde and 1% paraformaldehyde in 150 mM sodium cacodylate, pH 7.4 (all from Electron Microscopy Sciences, Hatfield, PA). The tissues were harvested as described for parotid salivary gland (Terasaki et al., 2013) and spinal cord (Furusho et al., 2017). The fixed tissues were processed by the ROTO protocol (Tapia et al., 2012), in which the tissue is incubated successively in reduced osmium, thiocarbohydrazide and unreduced osmium. The tissues were stained en bloc with uranyl acetate and then with lead aspartate (Walton, 1979), before using a standard protocol for dehydration with ethanol and infiltration with polybed resin (Polysciences, Warrington, PA), embedding and polymerization at 60 °C for 1-2 days.

The sections were cut on a Leica EM UC7 ultramicrotome (Leica, Buffalo Grove, IL) with a diamond knife (Diatome, Hatfield, PA) and collected with a custom built ATUM (automated tape collecting microtome) (Kasthuri et al., 2015). The tape containing the sections was cut into strips, mounted on 4 inch silicon wafers (University Wafers, South Boston, MA) and carbon coated (Denton 502B, Moorestown, NJ) to provide grounding for electron imaging.

The sections were imaged with a Verios field emission electron microscope (FEI, Hillsboro, OR) in backscatter mode (5 keV electrons, 0.4 nA beam current). The mapping and automated image collection was accomplished using the Matlab program SEM Navigator (kindly provided by Daniel Berger, Harvard) with some custom software modifications.

Images were aligned using the Linear Alignment with SIFT algorithm of FIJI Image J (<https://fiji.sc/>). Measurements were made using Image J.

## Acknowledgements

I thank Jeff Lichtman for help in getting started with the ATUM technique, discussions and noticing the little black dot in small axons, Richard Schalek for technical advice, and Daniel Berger for use of his program SEM Navigator. I also thank Miki Furusho for providing the spinal cord sample, Art Hand for preparing the salivary gland sample, Valentina Baena for sectioning and animating the axonal Er reconstruction, Maya Yankova for sectioning, and Tom Rapoport for discussions. Supported by a grant from the Connecticut Science Fund.

## References

- Aihara, Y., Inoue, T., Tashiro, T., Okamoto, K., Komiya, Y., and Mikoshiba, K.** (2001). Movement of endoplasmic reticulum in the living axon is distinct from other membranous vesicles in its rate, form, and sensitivity to microtubule inhibitors. *J. Neurosci. Res.* **65**, 236-246.
- Blackstone, C.** (2012). Cellular pathways of hereditary spastic paraplegia. *Annu. Rev. Neurosci.* **35**, 25-47.
- Denk, W., and Horstmann, H.** (2004). Serial block-face scanning electron microscopy to reconstruct three-dimensional tissue nanostructure. *PLoS Biol.* **2**, e329.
- Ellenberg, J., Siggia, E.D., Moreira, J.E., Smith, C.L., Presley, J.F., Worman, H.J., and Lippincott-Schwartz, J.** (1997). Nuclear membrane dynamics and reassembly in living cells: targeting of an inner nuclear membrane protein in interphase and mitosis. *J. Cell Biol.* **138**, 1193-1206.
- Fawcett, D.W.** (1981). *The Cell*. Philadelphia, PA: W.B. Saunders Co. 2nd edition. 862 pp.
- Furusho, M., Ishii, A., and Bansal, R.** (2017). Signaling by FGF Receptor 2, Not FGF Receptor 1, Regulates Myelin Thickness through Activation of ERK1/2-MAPK, Which Promotes mTORC1 Activity in an Akt-Independent Manner. *J. Neurosci.* **37**, 2931-2946.
- Grigoriev, I., Gouveia, S.M., van der Vaart, B., Demmers, J., Smyth, J.T., Honnappa, S., Splinter, D., Steinmetz, M.O., Putney, J.W. Jr, Hoogenraad, C.C., and Akhmanova, A.** (2008). STIM1 is a MT-plus-end-tracking protein involved in remodeling of the ER. *Curr. Biol.* **18**, 177-182.
- Hu, J., Shibata, Y., Voss, C., Shemesh, T., Li, Z., Coughlin, M., Kozlov, M.M., Rapoport, T.A., and Prinz, W.A.** (2008). Membrane proteins of the endoplasmic reticulum induce high-curvature tubules. *Science* **319**, 1247-1250.
- Jaffe, L.F.** (1977). Electrophoresis along cell membranes. *Nature* **265**, 600-602.

**Kasthuri, N., Hayworth, K.J., Berger, D.R., Schalek, R.L., Conchello, J.A., Knowles-Barley, S., Lee, D., Vázquez-Reina, A., Kaynig, V., Jones, T.R., Roberts, M., Morgan, J.L., Tapia, J.C., Seung, H.S., Roncal, W.G., Vogelstein, J.T., Burns, R., Sussman, D.L., Priebe, C.E., Pfister, H., and Lichtman, J.W.** (2015). Saturated reconstruction of a volume of neocortex. *Cell* **162**, 648-661.

**Lindsey, J.D., and Ellisman, M.H.** (1985). The neuronal endomembrane system. III. The origins of the axoplasmic reticulum and discrete axonal cisternae at the axon hillock. *J. Neurosci.* **5**, 3135-3144.

**Nixon-Abell, J., Obara, C.J., Weigel, A.V., Li, D., Legant, W.R., Xu, C.S., Pasolli, H.A., Harvey, K., Hess, H.F., Betzig, E., Blackstone, C., and Lippincott-Schwartz, J.** (2016). Increased spatiotemporal resolution reveals highly dynamic dense tubular matrices in the peripheral ER. *Science* **354**, 433.

**O'Sullivan, N.C., Jahn, T.R., Reid, E., and O'Kane, C.J.** (2012). Reticulon-like-1, the Drosophila orthologue of the hereditary spastic paraplegia gene reticulon 2, is required for organization of endoplasmic reticulum and of distal motor axons. *Hum. Mol. Genet.* **21**, 3356-3365

**Peters, A., Palay, S.L., and deF. Webster, H.** (1991). *The Fine Structure of the Nervous System*. Oxford University Press. 494 pp.

**Porter, K.R.** (1953). Observations on a submicroscopic basophilic component of cytoplasm. *J. Exp. Med.* **97**, 727-750.

**Porter, K.R., Claude, A., and Fullam, E.F.** (1945). A study of tissue culture cells by electron microscopy: methods and preliminary observations. *J. Exp. Med.* **81**, 233-246.

**Porter, K.R., and Blum, J.** (1953). A study in microtomy for electron microscopy. *Anat. Rec.* **117**, 685-710.

**Powers, R.E., Wang, S., Liu, T.Y., and Rapoport, T.A.** (2017). Reconstitution of the tubular endoplasmic reticulum network with purified components. *Nature* **543**, 257-260.

**Tapia, J.C., Kasthuri, N., Hayworth, K.J., Schalek, R., Lichtman, J.W., Smith, S.J., and Buchanan, J.** (2012). High-contrast en bloc staining of neuronal tissue for field emission scanning electron microscopy. *Nat. Protoc.* **7**, 193-206.

**Terasaki, M., Chen, L.B., and Fujiwara, K.** (1986). Microtubules and the endoplasmic reticulum are highly interdependent structures. *J. Cell Biol.* **103**, 1557-1568.

**Terasaki, M., Jaffe, L.A., Hunnicutt, G.R., and Hammer, J.A. 3rd.** (1996). Structural change of the endoplasmic reticulum during fertilization: evidence for loss of membrane continuity using the green fluorescent protein. *Dev. Biol.* **179**, 320-328.

**Terasaki, M., Shemesh, T., Kasthuri, N., Klemm, R.W., Schalek, R., Hayworth, K.J., Hand, A.R., Yankova, M., Huber, G., Lichtman, J.W., Rapoport, T.A., and Kozlov, M.M.** (2013). Stacked endoplasmic reticulum sheets are connected by helicoidal membrane motifs. *Cell* **154**, 285-296.

**Villegas, R., Martinez, N.W., Lillo, J., Pihan, P., Hernandez, D., Twiss, J.L., and Court, F.A.** (2014). Calcium release from intra-axonal endoplasmic reticulum leads to axon degeneration through mitochondrial dysfunction. *J. Neurosci.* **34**, 7179-7189.

**Voeltz, G.K., Prinz, W.A., Shibata, Y., Rist, J.M., and Rapoport, T.A.** (2006). A class of membrane proteins shaping the tubular endoplasmic reticulum. *Cell* **124**, 573-586.

**Walton, J.** (1979). Lead aspartate, an en bloc contrast stain particularly useful for ultrastructural enzymology. *J Histochem Cytochem* **27**, 1337-1342.

**Wu, Y., Whiteus, C., Xu, C.S., Hayworth, K.J., Weinberg, R.J., Hess, H.F., and De Camilli, P.** (2017). Contacts between the endoplasmic reticulum and other membranes in neurons. *Proc Natl Acad Sci U S A.* **114**, E4859-E4867.

Yalçın, B., Zhao, L., Stofanko, M., O'Sullivan, N.C., Kang, Z.H., Roost, A., Thomas, M.R., Zaessinger, S., Blard, O., Patto, A.L., Sohail, A., Baena, V., Terasaki, M., and O'Kane, C.J. (2017). Modeling of axonal endoplasmic reticulum network by spastic paraplegia proteins. *Elife* **6**, pii: e23882.

## Tables

Table 1. Changes in ER profile number per  $\mu\text{m}$

Tubules joining at branch	$2.12 \pm 0.81$
Tubules splitting at branch	$2.09 \pm 0.83$
Free end appear	$0.42 \pm 0.33$
Free end disappear	$0.49 \pm 0.30$

## Figures

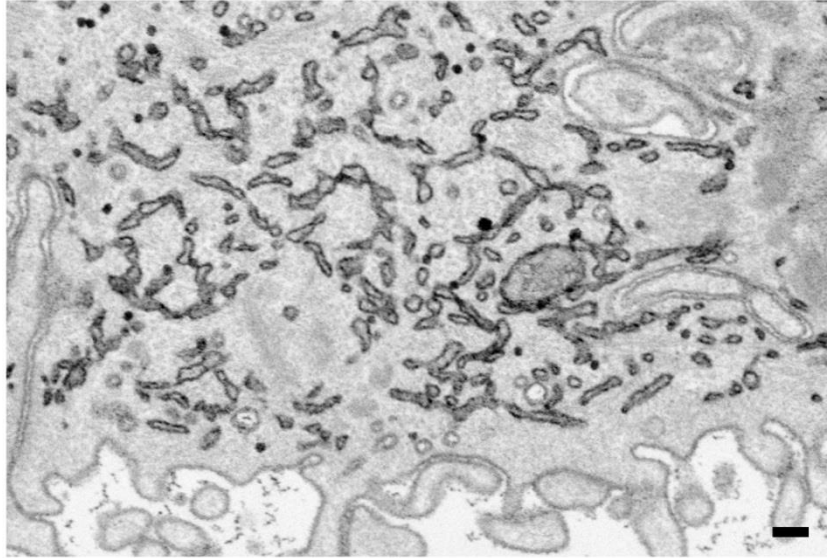


**Figure 1. A network of tubular ER in the apical region of an intercalated duct cell of mouse parotid salivary gland.** The tubule diameters are variable but many are ~60 nm, like the ER tubules in cells of most other tissues. Supplemental figure 1 shows the serial section sequence which contains this image. Bar, 200 nm.

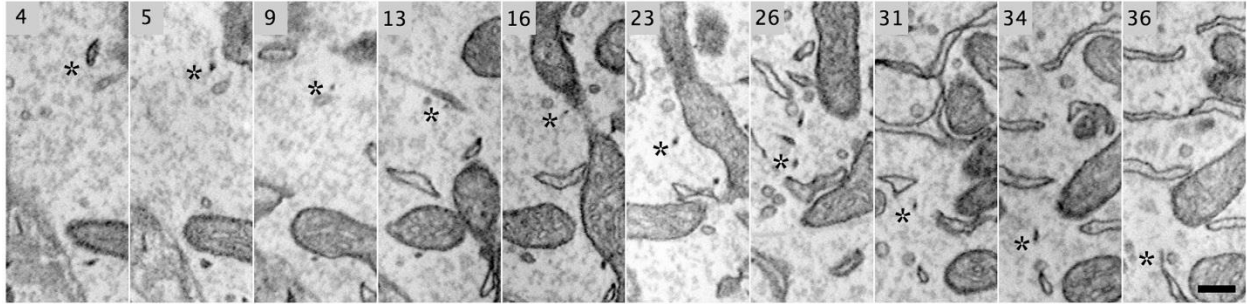


**Figure 2. A narrow ER tubule in a pyramidal neuron in the mouse cortex layer 4/5.** The diameter of this tubule varies from 15 to 30 nm in this sequence. The narrow tubule is unbranched and runs between ER tubules and sheets of wider diameter (to the right of the black asterisk in each panel). It is continuous with ER of wider diameter at both ends and its length is approximately 1 micron. The section number is displayed in the top left corner of each frame. Supplemental figure 2 shows the entire serial section sequence. Bar, 200 nm.

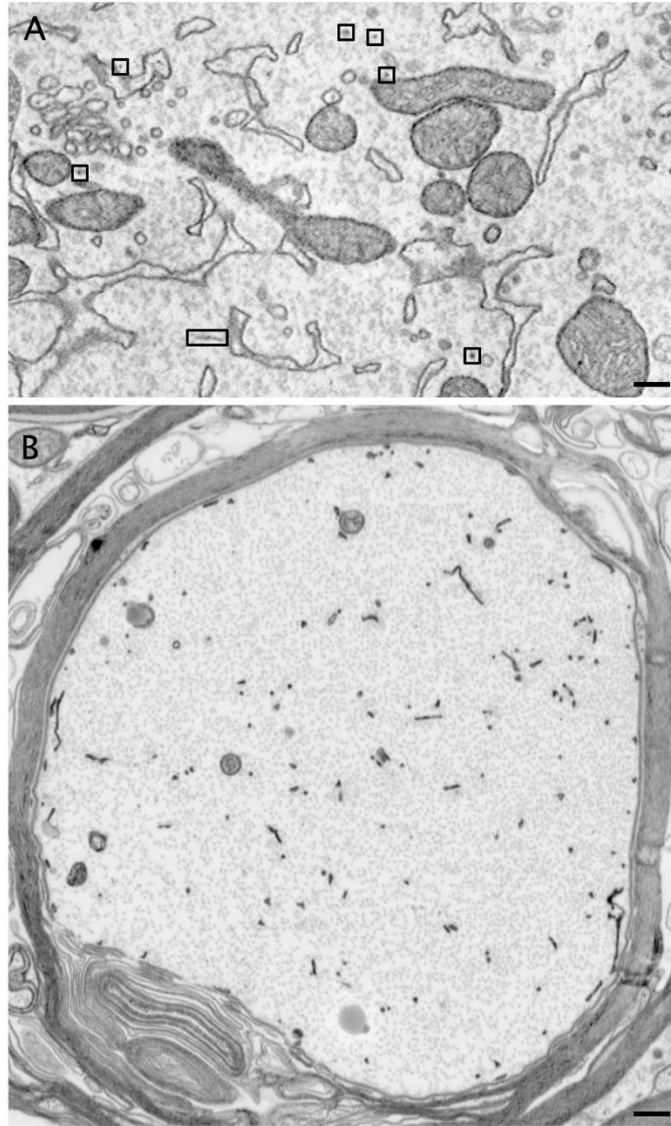


**Figure 3.** A) A region in the cell body of a pyramidal neuron in the mouse cortex layer 4/5. Most of the ER is a combination of cisternae and tubules of thickness comparable to that found in other cells, such as Figure 1. Narrow tubules such the one shown in Figure 2 are interspersed among this ER. Small black squares and rectangles indicate narrow tubules that were identified by inspecting the serial section image series of this region. Bar, 200 nm. B) A myelinated axon in the corticospinal tract of the mouse spinal cord. When viewed in serial section, the dark labeled membranes are all part of the ER. Essentially all of these tubular and sheet elements of the ER are narrow. This image is shown at the same magnification as Figure 3A. Supplemental figure 3 shows the serial section sequence which contains this image. Bar, 200 nm.

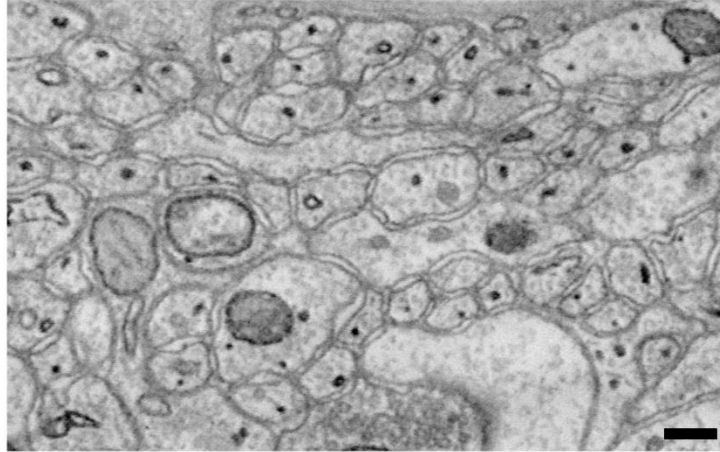


**Figure 4. Several small unmyelinated axons in mouse cortex layer 4/5 (arrows).** Each small axon has a single ER tubule in it that in serial section is usually narrow but occasionally widens. Supplemental figure 4 shows the serial section sequence which contains this image. Bar, 200 nm.

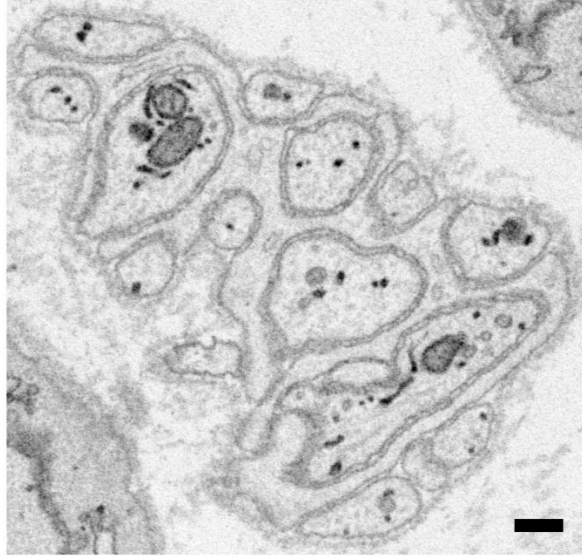


**Figure 5. A peripheral nerve containing several axons in the mouse parotid salivary gland.** In serial section, each nerve has a network of narrow ER tubules, just as in the central nervous system neurons seen in figures 3 and 4. Supplemental figure 5 shows the serial section sequence which contains this image. Bar, 200 nm.

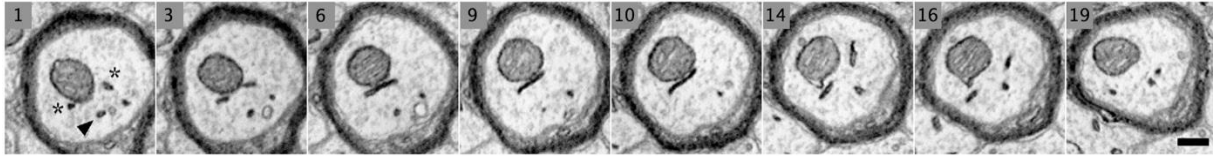


**Figure 6. Narrow tubule branching and a free end.** The section number is shown in the upper left corner of each frame. Two tubules are indicated by asterisks in section 1. These join to form a sheet in section 6, which then splits in section 14 to form two more tubules. The arrowhead in section 1 indicates another tubule, which disappears in section 10 indicating a free end. Bar, 200 nm.

Supplemental figure 6 shows the entire serial section sequence.

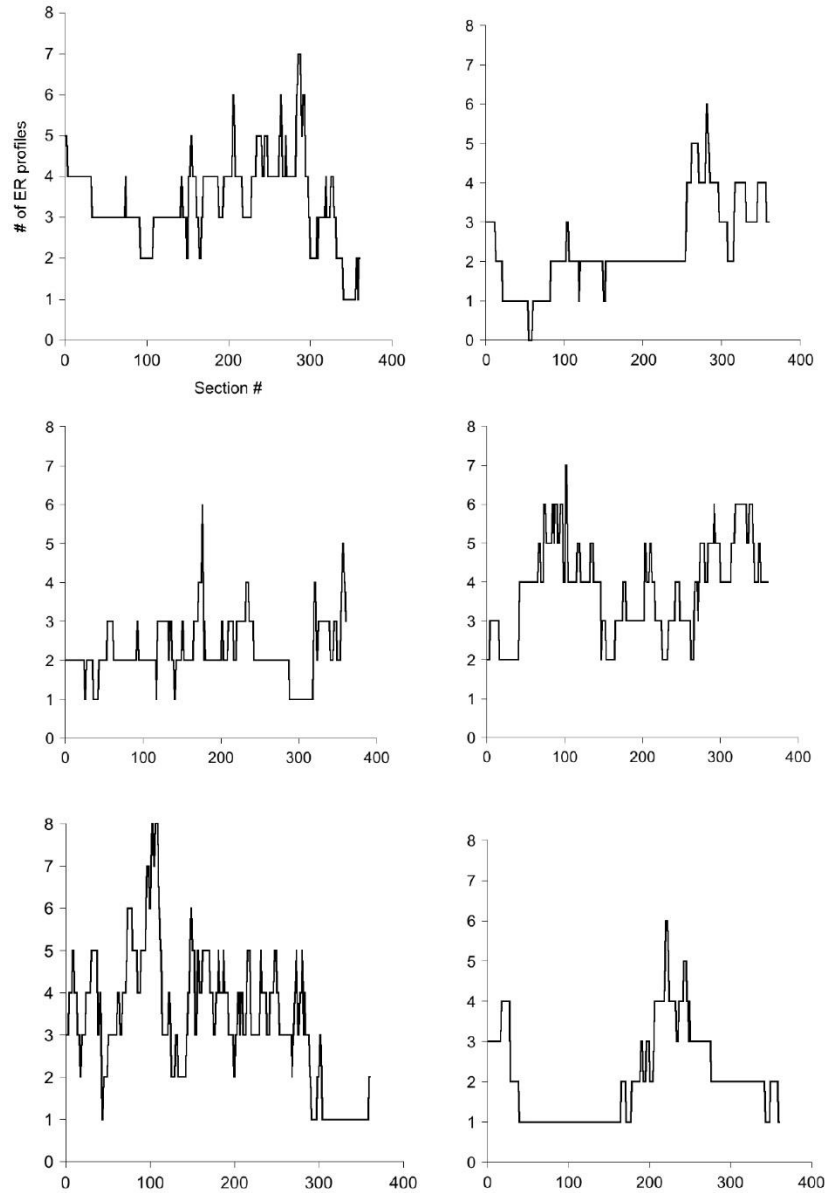
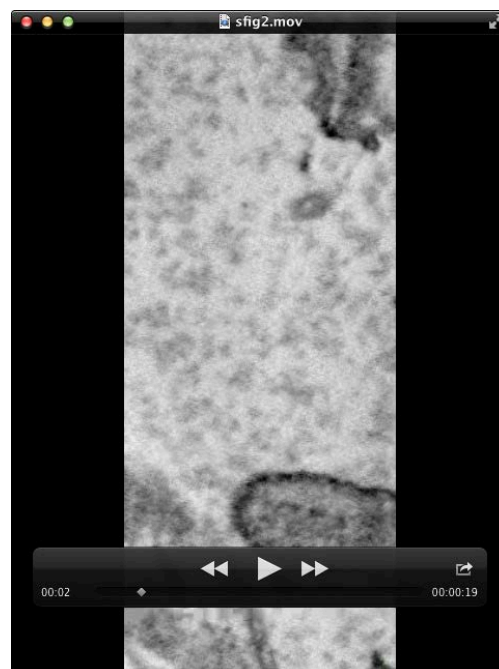


**Figure 7. The number of ER profiles in serial 30 nm thick sections of six small myelinated axons in layer 4/5 of cortex.** 360 sections from each axon was analyzed. The average cross sectional area was  $0.35 \pm 0.17 \mu\text{m}^2$ , with a diameter of  $0.67 \pm 0.18 \mu\text{m}$ . The anterograde / retrograde orientation of the axons is unknown so the direction of increasing section number was arbitrarily taken as the direction. For each panel, the number of ER profiles in the section is plotted on the y axis, and the section number is plotted on the x axis. Supplemental figure 7 shows the serial section series from the axon in the top right corner which has a gap in the ER continuity.

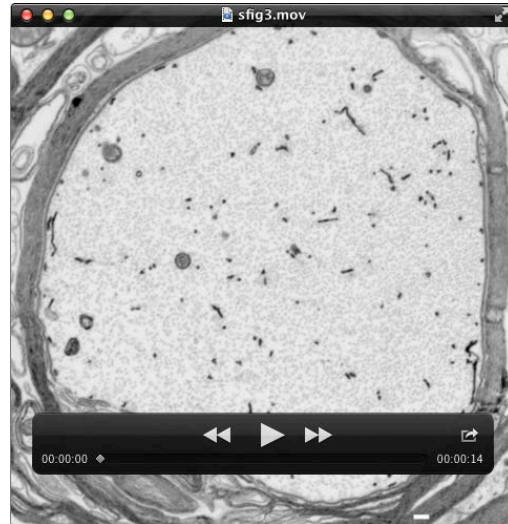
## Supplemental Movies



**Movie 1. Serial section sequence of the intercalated duct cell shown in Movie 1** (4.5 MB TIFF file, viewable in Image J). The sections were 35 nm thick and were imaged at 4 nm per pixel. In this figure, the image resolution was reduced to 8 nm per pixel. Bar, 200 nm.



**Movie 2. Serial section sequence of the thin ER tubule shown in Figure 2** (4.5 MB TIFF file). The thin tubule emerges at section 5 and connects at the other end at section 36. Several other narrow tubules are present. This sequence contains 38 sections (30 nm thick) imaged at 3 nm per pixel (Kasthuri et al., 2015). Bar, 200 nm.



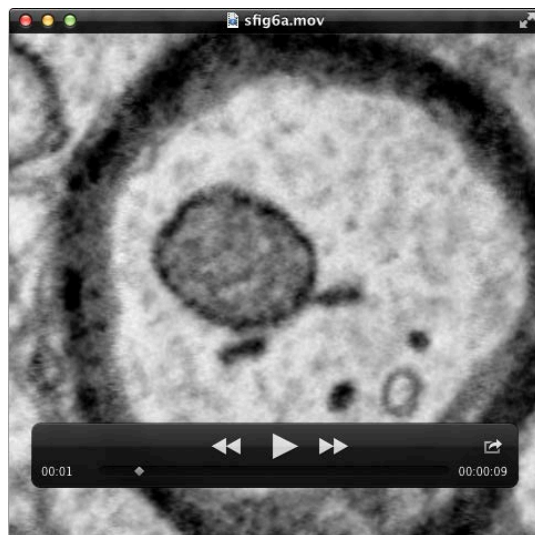
**Movie 3. Serial section sequence of the myelinated axon shown in Figure 3** (11.2 MB TIFF file). The original sequence contains 96 sections (60 nm thick) imaged at 3.5 nm per pixel. In this figure, the image resolution was reduced to 13.5 nm per pixel. Bar, 200 nm.



**Movie 4. Serial section sequence of the small axons shown in Figure 4** (7.3 MB TIFF file). The sections were 30 nm thick and imaged at 3 nm per pixel (Kasthuri et al., 2015). In this figure, the image resolution was reduced to 6 nm per pixel. Bar, 200 nm.



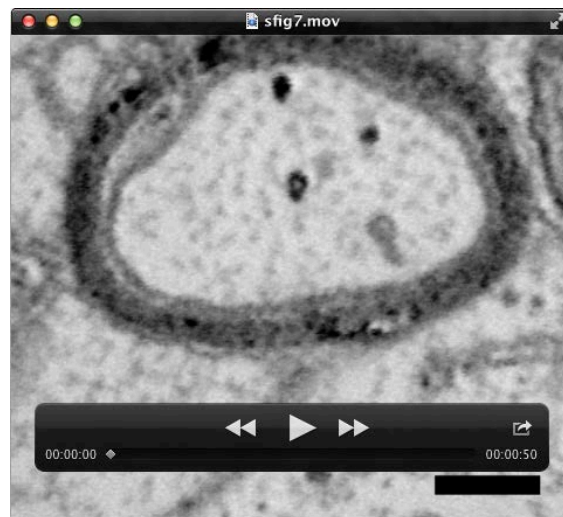
**Movie 5. Serial section sequence of the peripheral nerve shown in Figure 5** (9.1 MB TIFF file). The original sequence contains 68 sections (35 nm thick) imaged at 3 nm per pixel. In this figure, the image resolution was reduced to 6 nm per pixel. Bar, 200 nm.



**Movie 6A. Serial section sequence of the small myelinated axon shown in Figure 6** (1.9 MB TIFF file). This sequence contains 19 sections (30 nm thick) imaged at 3 nm per pixel. Bar, 200 nm.



**Movie 6B. Animated reconstruction of the ER in a small myelinated axon showing cisternae at branch points and free ended ER tubules.**



**Movie 7. Serial section sequence of the axon in the top right corner of Figure 7 (10.9 MB TIFF file). There are no ER profiles in frames 54 to 59, so there is a gap in the continuity of the ER in this axon. The sections were 30 nm thick and imaged at 3 nm per pixel (Kasthuri et al., 2015). The sequence that was analyzed contains 360 sections, and frames 1-122 are shown in this figure. Bar, 200 nm.**